

# Air Pollution Model Parameter Estimation Using Simulated LIDAR Data

James F. Kibler\* and John T. Suttles\*  
NASA-Langley Research Center, Hampton, Va.

One way to obtain estimates of the unknown parameters in a pollution-dispersion model is to compare the model predictions with remotely sensed air-quality data. A ground-based LIDAR sensor provides relative pollution-concentration measurements as a function of space and time. The measured sensor data are compared with the dispersion-model output through a numerical estimation procedure to yield parameter estimates that best fit the data. This overall process is tested in a computer simulation to study the effects of various measurement strategies. Such a simulation is useful prior to a field measurement exercise to maximize the information content in the collected data. Parametric studies of simulated data matched to a Gaussian plume-dispersion model indicate the trade offs available between estimation accuracy and data-acquisition strategy.

## Introduction

MANY air-pollution transport models have been developed to describe the way pollution from a variety of sources is moved through space and time. These models typically have several parameters as exponents or coefficients that must be empirically determined (for example, diffusion coefficients<sup>1</sup>). One way to obtain estimates of the unknown parameters in the pollution-transport models is to compare the model predictions with measured air-quality data. Since the values used for the parameters can markedly affect the model results, accurate estimates of the parameters must be obtained. The estimate accuracy, in turn, is affected by the data-gathering strategy used for air-quality measurements. Thus, it is important that alternative strategies be investigated to determine their effect upon the accuracy of the parameter estimates.

In this paper, a simulation of the overall parameter estimation technique is described. An air-pollution-transport model developed by Smith<sup>2</sup> is used as representative of the pollution-transport process. His model includes the effect of velocity shear in the wind field. Most Gaussian plume models assume a constant velocity field, which frequently produces results inconsistent with observed concentration profiles. For example, Johnson and Uthe<sup>3</sup> present plume cross sections measured by LIDAR (laser radar) which seem to exhibit effects due to a velocity shear with altitude. Thus, Smith's shear-diffusion model is more representative of atmospheric conditions that produce such shearing effects.

The data collection model is the next portion of this simulation study. Since the pollutant-transport model yields concentration as a function of spatial location, a concentration sensor must yield similarly compatible measurements. A ground-based LIDAR system<sup>4</sup> is an example of such a sensor. The LIDAR directs a pulsed laser beam at the pollutant plume and collects backscattered light with a telescope as a function of time. The amplitude of the returned signal can be related to the aerosol-pollution concentration and the time of flight determines the range along the line of sight. Thus, by knowing the position and orientation of the LIDAR with respect to the source, instantaneous values of concentration at a known location can be determined.

The final step in the simulation study is the estimation of values for the unknown model parameters in the system. Simulated measurements from the LIDAR model are processed by a weighted least-squares estimator<sup>5</sup> to obtain a set of model parameters that most closely matches the simulated data. The error between the estimated values and the assumed values for the model parameters provides an indicator of the accuracy of the estimation technique. Several parametric studies are presented to show the tradeoffs available between estimate accuracies and data acquisition strategy.

## Pollution-Transport Model

Smith<sup>2</sup> has developed three solutions to the general partial differential equation for pollutant transport in a nonuniform flow. The solutions are for an instantaneous point release, an instantaneous line release, and a steady-state point source. In this paper, his steady-state point source solution will be modified to serve as a representative pollution-transport model to use in simulating the parameter estimation technique.

First, assume that the velocity field is uniform in the  $x$  direction except for a dependence of the  $y$ -velocity component upon  $z$  (i.e., a crosswind velocity shear with altitude). Second, assume perfect reflection of the transported concentration from the ground. Third, assume a constant background concentration level exists that is independent of the pollutant source. Smith's solution for a unit source strength may then be written as

$$S = \beta + \frac{1}{2\pi u \sigma_y \sigma_z \left(1 + \frac{\Omega^2 \sigma_z^2}{12 \sigma_y^2}\right)} \exp \left\{ - \frac{\frac{y^2}{2\sigma_y^2} + \frac{(z \pm h_e)^2}{2\sigma_z^2} - \frac{\Omega y (z \pm h_e)}{2\sigma_y^2} \left[1 - \frac{\Omega (z \pm h_e)}{3y}\right]}{\left(1 + \frac{\Omega^2 \sigma_z^2}{12 \sigma_y^2}\right)} \right\} \quad (1)$$

where  $\Omega = (x/u) (\partial v / \partial z)$  and  $S$  is the pollution concentration,  $x, y, z$  is the position in the source coordinate system,  $\beta$  is background concentration,  $\sigma_y, \sigma_z$  are diffusion coefficients in the  $y$  and  $z$  direction,  $u, v$ , are  $x$  and  $y$  wind-velocity components,  $h_e$  is the effective source height above the  $x, y$  plane. Note that this solution reduces to the familiar time-averaged Gaussian plume model if there is no velocity shear ( $\partial v / \partial z = 0$ ).

Received Jan. 14, 1977; presented as Paper 77-75 at the AIAA 15th Aerospace Sciences Meeting, Los Angeles, Calif., Jan. 24-26, 1977; revision received July 6, 1977.

Index categories: Analytical and Numerical Methods; Simulation; Atmospheric and Space Sciences.

\*Aerospace Technologist. Member AIAA.

The diffusion coefficients,  $\sigma_y$  and  $\sigma_z$ , are dependent upon the distance from the source, so they may be modeled in turn as

$$\sigma_y = \sigma_{y0} x^a$$

$$\sigma_z = \sigma_{z0} x^b$$

More sophisticated models are available for the diffusion coefficients. However, the object is to express concentration as a function of parameters that may be assumed constant over all space. Introducing additional parameters merely complicates the notation.

Equation (1) describes the spatial transport of pollution concentration as a function of various model parameters. Figure 1 illustrates the effects of several of these parameters. For example,  $\sigma_y$  and  $\sigma_z$  influence the spread of concentration in the  $y$  and  $z$  directions;  $h_e$ ,  $u$ , and  $\sigma_z$  influence the downstream plume touchdown; and  $\partial v/\partial z$  influences the distortion in concentration levels as a function of  $y$ . If values for the parameters could be obtained, then the concentration model could be used to forecast or interpret pollution transport.

### LIDAR Sensor Model

The LIDAR is an instrument that emits a laser beam through the atmosphere and senses backscattered light. Since aerosols in the path of the laser reflect some portion of incident light, the return signal at the LIDAR can be related to the aerosol concentration along the light path. The time delay between firing the laser and collecting the returned signal determines the range of the aerosol concentration. Since concentration output from the transport model is a function of location in the source coordinate system, a transformation of the LIDAR output as a function of range is required.

Figure 2 illustrates the relative geometry of the source and the LIDAR in an inertial coordinate system. The source is located at  $X_s, Y_s$  and the LIDAR is located at  $X_m, Y_m, Z_m$ . The source coordinate frame  $(x, y)$  is oriented at an angle,  $\theta$ ,

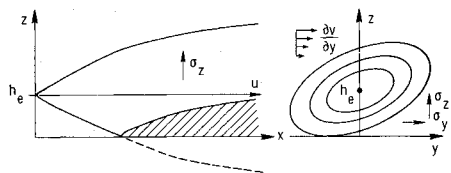


Fig. 1 Effect of several transport model parameters.

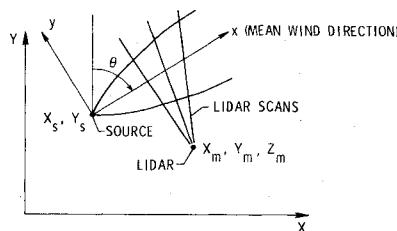


Fig. 2 Source and LIDAR location in an inertial coordinate system.

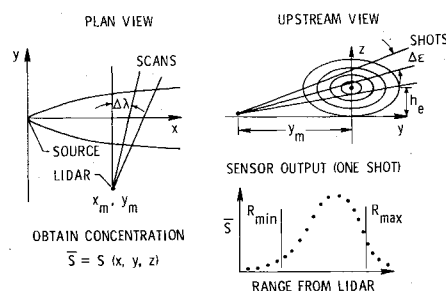


Fig. 3 LIDAR geometry in source coordinate system.

between  $Y$  and  $x$ , which is the direction of the mean wind. The LIDAR fires a sequence of shots at a constant azimuth,  $\lambda$ , with varying elevation,  $\epsilon$ . This scanning sequence is then repeated for various azimuths. The scan process is illustrated in Fig. 3. In that figure, the plan view shows different scans that vary in azimuth; the upstream view shows shots that vary in elevation; and the sensor output,  $\bar{S}$ , is shown as a function of range for a given shot.

Now, the transformation from range to position in the source reference frame is

$$x = R \cos \epsilon \cos(\theta - \lambda) + (X_m - X_s) \sin \theta + (Y_m - Y_s) \cos \theta \quad (2a)$$

$$y = R \cos \epsilon \sin(\theta - \lambda) - (X_m - X_s) \cos \theta + (Y_m - Y_s) \sin \theta \quad (2b)$$

$$z = R \sin \epsilon + Z_m \quad (2c)$$

where  $X_m, Y_m, Z_m$  is the location of the LIDAR,  $\epsilon, \lambda$  are the elevation and azimuth of the LIDAR shot,  $R$  is the range along the LIDAR shot,  $X_s, Y_s$  is the source location, and  $\theta$  is the orientation of the mean wind to an inertial reference frame.

Given this  $x, y, z$  position and an assumed set of transport model parameters,  $a$ , the transport model can be evaluated to yield concentration. Gaussian noise with zero mean and variance,  $\sigma_m^2$  can be added to the transport model output to yield a simulated measurement,

$$\bar{S}_i = S_i(a) + N(0, \sigma_m^2)$$

at the  $i$ th measurement location from Eq. (2). The noise represents both sensor errors and unmodeled transport characteristics.

Note that the transformation from sensor output as a function of range to the source reference frame introduces two additional sets of parameters:  $X_m, Y_m, Z_m, \epsilon, \lambda, R$  may be taken as measurement-dependent and may be varied to investigate alternative measurement strategies; and  $X_s, Y_s$ , and  $\theta$  may be assumed unknown, grouped with the transport-model parameters, and estimated from the simulated measurements.

### Parameter Estimation Procedure

The output of the transport model is pollution concentration as a function of spatial location and a set of unknown transport model parameters. On the other hand, the output of the LIDAR sensor model is pollution concentration as a function of spatial location, sensor characteristics, and assumed values for the transport model parameters. The next step, then, is to form estimates of the unknown transport model parameters that best fit the modeled sensor data. At the  $i$ th spatial location, the error in the fit of the measurements to the model,  $\delta_i$ , is

$$\delta_i = \bar{S}_i - S_i(a)$$

where  $a$  now represents the complete set of transport model parameters,

$$a^T = \left[ \sigma_{y0} \ a \ \sigma_{z0} \ b \ h_e \ X_s \ Y_s \ u \ \frac{\partial v}{\partial z} \ \theta \ \beta \right]$$

For the modeled concentration,  $S_i$ , to best match the measured concentration,  $\bar{S}_i$ , the model parameters,  $a$ , must be varied to minimize  $\delta_i$ . If an initial estimate of the model parameters is known,  $a_0$ , then  $\delta_i$  can be expanded and locally linearized to give

$$\delta_i \approx \bar{S}_i - S_i(a_0) - \frac{\partial S(a)}{\partial a} \bigg|_{a_0} \Delta a$$

Or, in vector notation,

$$\delta \approx \delta S - \Lambda \Delta a$$

where  $\delta$  is the vector of differences between the measured and modeled concentration at  $a$ ,  $\delta S$  is the vector of differences between the measured and modeled concentration at  $a_0$ ,  $\Lambda$  is the matrix of partial derivatives of concentration with respect to the model parameters, evaluated at  $a_0$ ,  $\Delta a$  is the vector of changes in the model parameters from  $a_0$ .

One way to minimize  $\delta$  is by the well-known weighted least-squares estimate

$$\Delta \hat{a} = (\Lambda^T W^{-1} \Lambda)^{-1} \Lambda^T W^{-1} \delta S \tag{3}$$

where

$$W = \begin{bmatrix} \sigma_1^2 & 0 & \dots & 0 \\ 0 & \sigma_2^2 & & \\ \cdot & & \cdot & \\ \cdot & & & \cdot \\ \cdot & & & \cdot \\ \cdot & & & \cdot \\ 0 & \cdot & \cdot & \cdot & \cdot & \cdot & \sigma_n^2 \end{bmatrix}$$

and  $\sigma_i^2$  is the variance of each of the different measurements which are assumed to be independent.

Then, the updated estimate of the model parameters is

$$\hat{a} = a_0 + \Delta \hat{a}$$

This procedure may be repeated by letting  $a_0 = \Delta \hat{a}$  is sufficiently small. The estimation procedure is illustrated in Fig. 4.

Using this procedure, Eq. (3) yields the best estimate of the unknown transport model parameters to fit the measured data. The term  $(\Lambda^T W^{-1} \Lambda)^{-1}$  represents the covariance of  $\Delta \hat{a}$ . The variance of each element of  $\Delta \hat{a}$  can be used as a figure of merit for evaluating alternative measurement strategies.

### Simulation Results

The pollution-transport and sensor models and the estimation procedure described previously have been programmed for a digital computer. Using the computer program, several parametric cases have been run to investigate alternative measurement strategies for the LIDAR sensor. The following standard strategy was chosen for comparison purposes: the LIDAR located at 1.5 km downstream and 2 km to the right of the wind vector; three LIDAR scans with the first normal to the plume and succeeding scans 10 deg to the right in azimuth; each scan composed of 10 shots

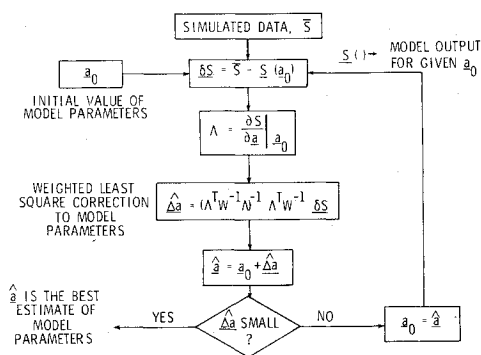


Fig. 4 Parameter estimation procedure.

with the first horizontal and succeeding shots 1 deg higher in elevation; and each shot discretized into 10 data points ranging from 1.5 to 2.5 km from the LIDAR. This strategy results in 300 values for concentration as a function of space. Typical values of the transport model parameters were used to generate the simulated measurements and Gaussian noise with variance approximately 1% of peak concentration was added to the measurements. For these parametric cases, a constant wind field with no velocity shear was used. The results of four different parametric cases are shown in Figs. 5-8. In each figure, the standard deviation of the parameter estimate is plotted vs the measurement variable of interest. Only selected results are plotted, but the trend of unplotted parameters is similar. Since the purpose of these figures is to illustrate trends in choosing a data gathering strategy, the absolute magnitude of the estimate standard deviations is unimportant.

The effect of varying the number of sequential scans is shown in Fig. 5. For this plot, the only variable in the data-

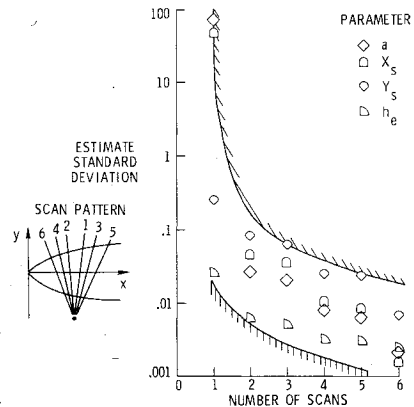


Fig. 5 Estimate standard deviation vs number of sequential scans.

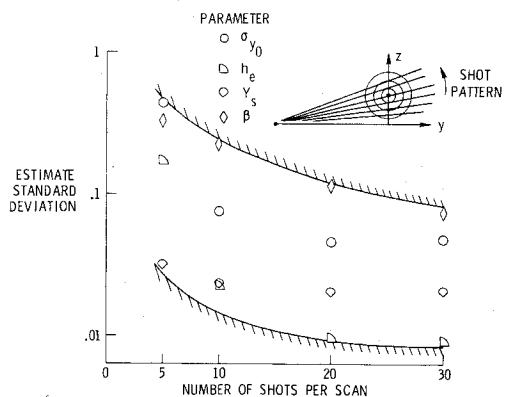


Fig. 6 Estimate standard deviation vs number of shots per scan.

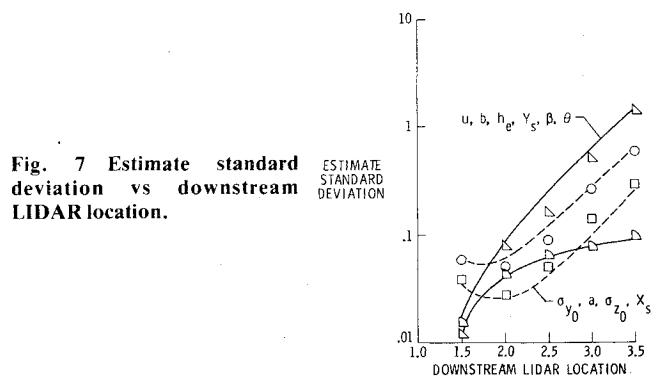


Fig. 7 Estimate standard deviation vs downstream LIDAR location.

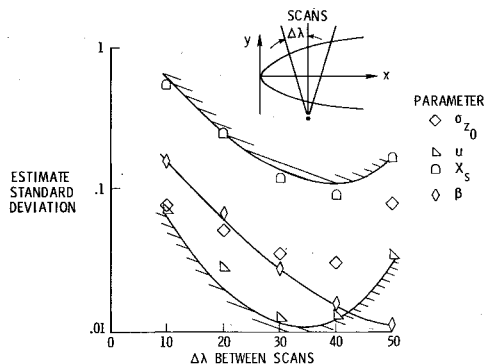


Fig. 8 Estimate standard deviation vs change in azimuth between scans.

gathering strategy is the number of LIDAR scans which varies from one to six sequential scans. The individual scans are labeled in the small diagram at the left and, for example, the 4-scan case would consist of scans 1, 2, 3, and 4. Note that a single scan has very high standard deviations and there is a general trend of better accuracy with increasing number of scans. The scans that are added away from the source have little impact, but the scans closer to the source significantly decrease the standard deviations. However, since there is a region near the source where unmodeled plume rise becomes important, scans very close to the source would provide no useful information for the model considered here. The definition of such a region would require analysis of actual data or a more sophisticated model that includes a plume rise formulation.

Figure 6 illustrates the effect of changing the number of shots per scan from 5 to 30. Again, the trend is toward lower standard deviations with increasing shots per scan. And again, after about 20 shots per scan, there is little improvement in estimate accuracy.

The importance of downstream LIDAR location is shown in Fig. 7. Here there are two different groupings in the behavior of the parameter estimates. One group ( $u$ ,  $b$ ,  $h_e$ ,  $Y_s$ ,  $\beta$ ,  $\theta$ ) has consistently higher standard deviations as the

downstream LIDAR location varies from 1.5 to 3.5 km. The other group ( $\sigma_{y_0}$ ,  $a$ ,  $\sigma_{z_0}$ ,  $X_s$ ) exhibits a minimum standard deviation at a downstream location of approximately 2 km. Thus, there is clearly a tradeoff available depending upon which group is required to be more accurately estimated.

Finally, Fig. 8 shows the effect of increasing the azimuth spread between scans. The strategy is sketched at the top of the figure and shows the standard three-scan case but with the center scan always perpendicular to the plume and the outer two scans spread by  $\Delta\lambda$ . Here, one parameter ( $\beta$ ) shows a consistent decrease in its estimate standard deviation as the azimuth spread varies from 10 to 50 deg. Since the remaining parameters exhibit a minimum near 30-40 deg, they can be more accurately estimated if such spacing is used in the scanning strategy.

### Concluding Remarks

A parameter estimation technique has been simulated for a ground-based LIDAR sensor using a representative air-pollution-transport model. Using an estimation procedure similar to this, the experiment designer may investigate alternative data-gathering strategies prior to using valuable resources in a field measurement exercise. Typical parametric cases have been presented to indicate the types of tradeoffs available to the experiment designer. A premission simulation such as the one described here should be a prerequisite to every field measurement with a new sensor type.

### References

- Turner, D.B., "Workbook of Atmospheric Dispersion Estimates," EPA Publication AP-26, July 1971.
- Smith, G.L., "Pollutant Dispersal in a NonUniform Flow," *Third Symposium on Atmospheric Turbulence, Diffusion, and Air Quality*, Raleigh, N.C., Oct. 1976.
- Johnson, W.B. and Uthe, E.E., "LIDAR Study of the Keystone Stack Plume," *Atmospheric Environment*, Vol. 5, 1971, pp. 703-724.
- Uthe, E.E. and Allen, R.J., "A Digital Real-Time Lidar Data Recording, Processing, and Display System," *Optical and Quantum Electronics*, Vol. 7, 1975, pp. 121-129.
- Liebelt, Paul B., *An Introduction to Optimal Estimation*, Addison-Wesley, Reading, Mass., 1967.